Experimental verification of theoretical equations for acoustic radiation force on compressible spherical particles in traveling waves

Kennita A. Johnson, Hannah R. Vormohr, Alexander A. Doinikov, Ayache Bouakaz, C. Wyatt Shields, IV, Gabriel P. López, and Paul A. Dayton

Phys. Rev. E **93**, 053109 — Published 17 May 2016

DOI: 10.1103/PhysRevE.93.053109

Experimental Verification of Theoretical Equations for Acoustic Radiation Force on Compressible Spherical Particles in Traveling Waves

Kennita A. Johnson,[1,2,*] Hannah R. Vormohr,[3] Alexander A. Doinikov,[4] Ayache Bouakaz,[4]
C. Wyatt Shields IV,[2,5] Gabriel P. López,[2,5,6] and Paul A. Dayton[1]

[1]*Joint Department of Biomedical Engineering, University of North Carolina at Chapel Hill, Chapel Hill, NC 27599*
[2]*NSF Research Triangle Materials Research Science and Engineering Center, Durham, NC 27708*
[3]*Departments of Chemistry and Biology, University of Indianapolis, Indianapolis, IN 46227*
[4]*INSERM U930, Université François Rabelais, 37032 Tours, France*
[5]*Department of Biomedical Engineering, Duke University, Durham, NC 27708*
[6]*Department of Mechanical Engineering and Materials Science, Duke University, Durham, NC 27708*
**Corresponding author, kennita@email.unc.edu*

ABSTRACT

Acoustophoresis uses acoustic radiation force to remotely manipulate particles suspended in a host fluid for many scientific, technological and medical applications, such as acoustic levitation, acoustic coagulation, contrast ultrasound imaging, ultrasound-assisted drug delivery, etc. To estimate the magnitude of acoustic radiation forces, equations derived for an inviscid host fluid are commonly used. However, there are theoretical predictions that, in the case of a traveling wave, viscous effects can dramatically change the magnitude of acoustic radiation forces, which make the equations obtained for an inviscid host fluid invalid for proper estimation of acoustic radiation forces. To date, experimental verification of these predictions has not been published. Experimental measurements of viscous effects on acoustic radiation forces in a traveling wave were conducted using a confocal optical and acoustic system and values were compared with available theories. Our results show that, even in a low-viscosity fluid such as water, the magnitude of acoustic radiation forces is increased many-fold by viscous effects in comparison with what follows from the equations derived for an inviscid fluid.

I. INTRODUCTION

Acoustic radiation forces are acoustically induced hydrodynamic forces that can cause particles suspended in a host fluid to migrate or cluster at certain regions [1]. This phenomenon is an integral part of many recent scientific, technological and medical applications, such as for imaging [2–7], colloidal assembly [8] and various bioseparation assays [9–11]. As new materials with advanced properties are developed for these applications (e.g., compressible particles), it is critical to understand their physical properties to accurately estimate their behavior in acoustic fields using theoretical relations. Commonly, in the estimation of acoustic forces incident on particles, equations derived for an inviscid host fluid are used. These equations do not take into account the viscous effects, even in low dissipative fluids like water. As such, various theoretical equations describing acoustic radiation forces incident on compressible, spherical particles in viscous host media have been reported to predict the force on such a particle with radius, R, and density, ρ_p, in an acoustic field of angular frequency, ω, and pressure amplitude, P [12–14]. While there are several prominent theoretical models to estimate these radiation forces, experimental verification has not been published to date.

The purpose of this report is to experimentally demonstrate that the viscosity of the host liquid cannot be ignored when calculating acoustic radiation forces. We have devised a simple experimental setup to measure the magnitude of acoustic radiation forces acting on individual semi-compressible spheres (i.e., polystyrene; bulk modulus of ~4 GPa [15]) in different fluids with a range of viscosities. We then evaluate the predicted force acting on polystyrene particles of a certain size using four prominent theoretical models and the known physical

properties of bulk polystyrene. We consider the effects of radiation force on the particle as a function of the frequency of the acoustic wave, particle size and dynamic viscosity. Finally, from our results, we compare these models and provide new insights on the accuracy of each model for a variety of conditions.

II. BACKGROUND

King [16] was among the first to rigorously define an equation for the acoustic radiation force on a particle, which was for a rigid sphere in a traveling wave in an inviscid fluid. The acoustic wavelength, λ_s, is related to f (the frequency of the acoustic wave) and c_0 (the speed of sound in the host media) by $\lambda_s = c_0/f$. In the limiting case, where the size of the particle is very small compared to the acoustic wavelength, λ_s ($k_0R << 1$, where k is the wave number), the acoustic radiation force, F_{Rad}, from this model is shown by:

$$F_{Rad} = \frac{2\rho_o P^2 \omega^6 R^2}{{c_0}^6}\left[\frac{1+\frac{2}{9}\left(1-\frac{\rho_0}{\rho_p}\right)^2}{\left(2+\frac{\rho_0}{\rho_p}\right)^2}\right], \tag{1}$$

where ρ_0 and ρ_p are the densities of the host fluid and particle, respectively, angular frequency, $\omega = 2\pi f$.

Yosioka and Kawasima [17] expanded this theory by considering the acoustic radiation force on a compressible, spherical particle in an inviscid fluid. The limiting case for Eq. (2) is that $(k_0R)^2$ and $(k_pR)^2$ are negligibly small, k_0 and k_p are the wave number of the host fluid and particle, respectively. This model, shown in Eq. (2), introduces the speed of sound in the particle, c_p, which is related to the compressibility of the particle, β_p ($c_p = \sqrt{1/\beta_p\rho_p}$):

$$F_{Rad} = \frac{2\pi P^2 \omega^4 R^6}{9\rho_0\left(2+\rho_o/\rho_p\right)^2 c_0^6}\left\{\left[3-\left(2+\frac{\rho_0}{\rho_p}\right)\frac{\rho_0 c_0^2}{\rho_p c_p^2}\right]^2 + 2\left(1-\frac{\rho_0}{\rho_p}\right)^2\right\}. \tag{2}$$

Danilov and Mironov [12] later developed a theoretical equation for compressible spherical particles in viscous media. This theory incorporated a term for the so-called viscous penetration depth, $\delta_\nu = \sqrt{2\nu/\omega}$, which is the boundary around the particle of a certain size that depends on both the kinematic viscosity of the host media, ν, and ω. The dynamic viscosity, η, is related to ν through the relation $\nu = \eta/\rho$, where ρ is the density of the viscous material, in the cases presented here would correspond to the host fluid. The thickness of this boundary layer plays an important role in the magnitude of the acoustic radiation force on particles. Similar to the previous models, this model, shown in Eq. (3), is valid in the limiting case where the radius of the particle is small compared to the wavelength of sound:

$$F_{Rad} = \frac{6\pi\nu R P^2}{\rho_0 c_0^3}\frac{\left(1-\frac{\rho_p}{\rho_0}\right)^2\left(1+\frac{\delta_\nu}{R}\right)}{\left(1+\frac{\rho_p}{2\rho_0}+\frac{9\rho_p\delta_\nu}{4\rho_0 R}\right)^2+\left(\frac{9\rho_p\delta_\nu^2}{4\rho_0 R^2}\right)^2\left(1+\frac{R}{\delta_\nu}\right)^2}. \tag{3}$$

Doinikov [13] formulated theoretical equations for compressible sphere in viscous fluid under two limiting cases (i.e., strong dissipation ($R << \delta_\nu << \lambda_s$) and weak dissipation ($\delta_\nu << R << \lambda_s$)), as described by Eq. (4). This theory shows that the influence of viscosity on the radiation force is determined by the parameter δ_ν/R. As $\delta_\nu/R \rightarrow 0$, Eq. (2) is appropriate, but if δ_ν/R is not negligibly small, viscous effects cannot be ignored. Eq. (4) has different dependence on ω and R than Eq. (2) and predicts that the magnitude of the radiation force is much larger than that given by Eq. (2):

$$F_{Rad} = \frac{6\sqrt{2}\pi P^2 \left(1 - {\rho_0}/{\rho_p}\right)^2 R^2 \sqrt{\omega\nu}}{\rho_0 \left(2 + {\rho_0}/{\rho_p}\right)^2 c_0^3}. \quad (4)$$

Settnes and Bruus [14] recently added to the field of knowledge the limiting case where δ_v and R are small compared to the size of the wavelength, but are on the same order of magnitude as each other. This limiting case, as shown by Eq. (5), is important in modern applications like microchannel acoustophoresis [18] of compressible particles in viscous fluids:

$$F_{Rad} = \frac{3\pi R^3 \omega P^2}{\rho_0 c_0^3} \left(\frac{\left(1 - \frac{\rho_p}{\rho_0}\right)^2 \left(1 + \frac{\delta_v}{R}\right)\frac{\delta_v}{R}}{\left(1 + 2\frac{\rho_p}{\rho_0}\right)^2 + 9\left(1 + 2\frac{\rho_p}{\rho_0}\right)\frac{\delta_v}{R} + \frac{81}{2}\left(\frac{{\delta_v}^2}{R^2} + \frac{{\delta_v}^3}{R^3} + \frac{{\delta_v}^4}{2R^4}\right)} \right). \quad (5)$$

These models (summarized in Table I) are by no means an exhaustive report of models used to describe acoustic radiation forces from a traveling wave, but they represent the leading models used to describe the major theoretical developments for acoustic radiation forces from a traveling wave on a compressible, spherical particle.

III. METHODS AND SETUP

A. Opto-acoustic system

The total force (F_{Total}) on a particle suspended in a viscous fluid subject to an acoustic wave includes the viscous drag force F_{Drag} [19]. As the particle is displaced by acoustic radiation forces, F_{Rad}, F_{Drag} acts on the particle in the opposite direction. The particle is accelerated by F_{Rad} until it reaches a terminal velocity. When the acceleration is zero, the net force is equal to zero ($F_{\text{Total}} = F_{\text{Rad}} + F_{\text{Drag}} = 0$), which means the magnitude of the acoustic radiation force is equal to the magnitude, or the absolute value, of the drag force ($F_{\text{Rad}} = -F_{\text{Drag}}$). This assumes that Brownian motion as well as gravity and buoyancy are negligible. In the experiments conducted herein, measurements were taken under this equilibrium condition, which permitted the use of the drag force as an estimate of the acoustic radiation force.

The experimental setup used an unconstrained opto-acoustic system (Fig. 1), which has been described previously [20, 21]. The unconstrained opto-acoustic experimental setup permits the particles to move without the limitation of physical boundaries. An essential test condition for this study was that the velocity of the particle must be measured once the acceleration equals zero. Confining particles to an optically transparent tube or other physical boundaries would limit the particles ability to reach terminal velocity. By allowing the particles to freely pass through the confocal optical and acoustic fields, the high-speed camera was able to capture the unhindered motion of the particles displaced by acoustic radiation force.

A large water tank was designed to accommodate a 100X water immersion objective (LUMPlanFl, NA=1.0; Olympus, Center Valley, PA, USA) coupled to a high-speed camera (FastCam, SA1.1, Photron USA, Inc., San Diego, CA, USA) to track the deflection of particles in response to the traveling pressure wave. The tip of a calibrated needle hydrophone (HNA-0400, Onda Corp., Sunnyvale, CA, USA) was adjusted until it was optically focused. Ultrasound transducers were positioned in such a way that the signal received by the hydrophone was maximized. Four spherically focused transducers (Panametrics, Inc., Waltham, MA, USA: 1.0 MHz [V314], 2.25 MHz [V305], 5.0 MHz [V308] and 7.5 MHz [V321]) were employed, and each had a diameter of 0.75 inches and a focal distance of 2.0 inches. Once the optical and acoustic foci were aligned, the hydrophone was removed. A particle injector was constructed by connecting a 27-gauge blunt needle (CML Supply LLC, Lexington, KY, USA) to a syringe using polyethylene 20 tubing (Becton, Dickinson and

Company, Franklin Lake, NJ, USA). The tip of the particle injector was positioned so that the particles flowed through mutual optical and acoustic foci (Fig. 1).

The system was configured in order to synchronize the video capture with the ultrasound pulse. Briefly, an arbitrary waveform generator (AFG 3101, Tektronix, Inc., Beaverton, OR, USA) was used to trigger both the video capture and a sinusoid pulse signal 50,000 cycles in length to the amplifier (3200L, E&I, Rochester, NY, USA) connected to the transducer. The video capture was computer controlled by Fastcam Viewer software (Photron USA, Inc., San Diego, CA, USA) at a rate of 5,000 frames per second in an optical field that was 768 pixels x 768 pixels at a resolution of 5.33 pixels per micron.

To ensure that the acoustic field in the experimental measurements would be an acceptable comparison to the traveling plane wave in the theoretical equations, the acoustic field for each transducer was mapped with the calibrated hydrophone. The optical field of view was 0.14 mm height x 0.14 mm wide. The width of acoustic field produced by the circular transducer was defined by the acoustic pressure at −3 dB in the lateral direction, which was measured to be 3.4, 2.1, 1.1 and 0.6 mm at the focus for the 1.0, 2.25, 5.0 and 7.5 MHz transducers, respectively. The length of the acoustic field in the axial direction was on the order of millimeters for all transducers used. The variation of the acoustic field is less than 1 dB inside the optical field of view, even at the highest frequency tested. Since the acoustic field is uniform within the optical field, of view and the diameter of the particles is much smaller than the optical field of view, the acoustic field produced by the circular focused transducers is an acceptable comparison to plane traveling wave at the location where the radiation force was measured.

B. Experimental measurements

Three experiments were conducted to test the force dependence on frequency, particle size and host fluid viscosity. In the first experiment (i.e., frequency as the independent variable), polystyrene beads (2.10 μm diameter; Spherotech, Inc., Lake Forest, IL, USA) were diluted with distilled water in the syringe and injected into the water bath through the optical focus using a calibrated syringe pump (PHD2000, Harvard Apparatus, Holliston, MA, USA) at a rate of 5 μl/hr. The viscosities of the host fluids were measured using a protocol described previously [22]. The host fluid was distilled water (dynamic viscosity, η = 0.001 Pa s). For each frequency (1.0, 2.25, 5.0 and 7.5 MHz), a minimum of five videos was saved. In the second experiment (i.e., particle size as the independent variable), the transducer parameters were kept constant at a frequency of 7.5 MHz and pulse length of 50,000 cycles. The diameters of the polystyrene particles injected into the water bath were varied (2.10, 5.52 and 8.04 μm; Spherotech, Inc., Lake Forest, IL, USA). The host fluid was distilled water. The third experiment (i.e., host fluid viscosity as the independent variable) used the same ultrasound parameters as the previous experiment and the diameter of the particles was held constant at 2.10 μm. The dynamic viscosity of the host fluid was increased by dissolving different amounts of ultrasound gel (Aquasonic Clear, Parker Laboratories, Inc., Fairfield, NJ, USA) in distilled water. The dynamic viscosities of the host fluids were 0.0010, 0.0015, 0.0026 and 0.0031 Pa s. For each of the three experiments, the pressure amplitude of the ultrasound signal at the mutual acoustic/optical foci was measured using the calibrated needle hydrophone.

Video captures were analyzed off-line with *ImageJ* software (NIH, Bethesda, MD, USA) with the plugin *MTrackJ* [23] to determine the velocity of the displaced particles. Fig. 2 is a representative image of the particle motion caused by acoustic radiation force. This image was created by taking the sum of the frames of the video clips saved from the high-speed camera such that the entire video sequence is displayed in one image. The particle motion can be seen as "particle tracks" as the particle floats upward after it has been ejected from the particle injector placed just below the optical field. For each experimental condition described above, 15 particle tracks were analyzed. Prior to the ultrasound pulse, particles traveled upward in the vertical direction (Fig. 2(a)). When the ultrasound was on, the particles were displaced by the acoustic wave incident perpendicular to the upward motion (Fig. 2(b)). As a result, the particles deviated from their vertical path by the angle θ. The horizontal component of the terminal velocity caused by F_{Rad} was determined as $v_{\mathrm{rad}} = v_p \cdot \sin\theta$,

where v_p is the velocity of the particle. Once the ultrasound pulse is terminated, the particle continues to move upward (Fig. 2(c)). Since the Reynolds numbers for the particles were very small, the terminal velocities were substituted into the Stokes' drag equation ($F_{Drag} = 6\pi\eta R \cdot v_{rad}$) to calculate the magnitude of F_{Drag}, which was used as an estimate of the acoustic radiation force experienced by the particles.

C. Quantitative analysis

A quantitative assessment was performed to determine which theoretical equation most closely estimated the acoustic radiation force measured in the experiment. First, the absolute value of the difference between the experimental and the corresponding theoretical value was calculated for each experimental time point. The average of the difference was taken for each theoretical equation used in all three types of experiments. The theoretical equation with the lowest average difference was considered the best predictor and the largest average difference was considered the worst predictor.

IV. RESULTS AND DISCUSSION

The experimental forces determined by Stokes' law were compared to the theoretical values from Eqs. (2) through (5). Eq. (1) was removed from the analysis because it assumes the particles are perfectly rigid. We compare theories of compressible particles in a viscous fluid (Eqs. (3), (4) and (5)) to compressible particles in an inviscid fluid (Eq. (2)). The Reynolds numbers (Table II) are sufficiently small; therefore, the F_{Drag} can be used in this instance. When calculating the force from the theoretical equations, the values for the variables were matched to the experimental conditions. Each model defined the limiting case where the physics described by the equation was appropriate. The limiting cases were based on assumptions made when deriving the equations from the theoretical interaction between the particle, host fluid and acoustic wave. Table II lists the values for λ_s, δ_v and k_0R in order to determine if the experimental circumstances fell within the limiting case for each theoretical equation.

A. Variable ultrasound frequency

We compared the forces from theoretical and experimental data to frequency (Fig. 3), radius (Fig. 4) and viscosity (Fig. 5). The dependence of each equation on those variables is detailed in Table III. Fig. 3, a representative semi-log plot of force vs. frequency, illustrates how the model from Eq. (2) dramatically underestimates the acoustic radiation force acting on each particle. Data for other acoustic pressures measured were similar. The forces calculated from Eqs. (3), (4) and (5) were on the same order of magnitude as the experimental data, confirming that viscous effects cannot be ignored. Although F_{Drag} is frequency independent, the viscous penetration depth is dependent on angular frequency, $\omega^{-1/2}$. The experimental data most closely matches the prediction by Eq. (4), suggesting that the acoustic radiation force has a dependence of $\omega^{1/2}$.

B. Variable particle radius

The second experiment compared the forces versus the change in particle radius. Fig. 4 shows how Eqs. (4) and (5) converge on to the inviscid host fluid scenario reflected in Eq. (2) as the values of δ_v/R decrease for larger radii (Table II). The trend in the experimental data is similar to that of the prediction by Eq. (3), but with the experimental values being larger by some scalar quantity. This is not surprising since the experimental data was calculated using F_{Drag}, which depends on radius, R, like in Eq. (3).

C. Variable host fluid viscosity

In the final experiment, the forces were measured with increasing host fluid viscosity (Fig. 5). Since there is no accounting for viscosity in Eq. (2), it remained unchanged as the frequency and radius were held constant for all experimental conditions. The experimental data is on the same order of magnitude as Eqs. (3), (4) and (5). It should be noted that the limiting case for Eq. (4), $\delta_v << R << \lambda_s$, may not have been satisfied by the experimental conditions, since δ_v is only one order of magnitude lower than R. This may become more exaggerated with increasing host fluid viscosity. Also, note that the limiting case for Eq. (3) does not have any specifications on viscosity. The limiting case for Eq. (5), $\delta_v, R << \lambda_s$, is more appropriate for the experimental conditions. Although no theory matched experimental data perfectly, Eq. (5) had the lowest average error in the experiment where viscosity of the host fluid was increased. This suggests that the dependence of acoustic radiation force on viscosity is similar to that of the prediction by Eq. (5).

V. CONCLUSION

Accurate characterization of forces is essential in applications that rely on acoustic waves for remote manipulation of particles. The work performed here provides verification that viscous effects cannot be neglected even in low-viscosity fluids. Estimates of acoustic radiation forces on particles in traveling waves will be grossly underestimated in cases where host fluids are considered inviscid. No single theory completely characterized the effect of changing acoustic frequency, particle radius and host fluid viscosity of the force incident on a small particle from an acoustic traveling wave. Each theory that included viscous effects (Eqs. (3), (4) and (5)) had it strengths reliant on which of the dependent variables (ω, R or η) was varied. When using these theories to predict forces, care should be taken match the limiting cases to the experimental conditions. In the future, other limiting cases should be investigated such as the case under strong dissipation where rigid spheres would move in the opposite direction of wave propagation [1]. The confocal opto-acoustic experimental setup allowed for the visualization and quantification of the behavior of particles immersed in a viscous fluid, whose motion was influenced by acoustic traveling waves. This experimental setup also provides a means to investigate the acoustic properties new materials developed for acoustophoretic applications.

ACKNOWLEDGEMENTS

We thank D. Hill for assistance with the viscosity measurements, S. Kasoji and J. Rojas for assistance with the construction of the experimental apparatus as well as B. Lindsey, K. H. Martin and A. Novell for assistance with the acoustic measurements. This research was supported by the National Science Foundation Research through the Materials Interdisciplinary Research Team (MIRT) Summer REU Program (DMR-1122483), the Research Triangle MRSEC (DMR-1121107) and a Graduate Research Fellowship (1106401) to C.W.S.

REFERENCES

[1] A. Doinikov, Recent Res. Devel. Acoust. **1**, 39 (2003).
[2] R. C. Gessner, J. E. Streeter, R. Kothadia, S. Feingold, and P. A. Dayton, Ultrasound Med. Biol. **38**, 651 (2012).
[3] M. A. Borden, J. E. Streeter, S. R. Sirsi, and P. A. Dayton, Mol. Imaging **12**, 357 (2013).
[4] K. Nightingale, M. S. Soo, R. Nightingale, and G. Trahey, Ultrasound Med. Biol. **28**, 227 (2002).
[5] A. V Patil, J. J. Rychak, J. S. Allen, A. L. Klibanov, and J. A. Hossack, Ultrasound Med. Biol. **35**, 2021 (2009).
[6] T. J. Czernuszewicz, J. W. Homeister, M. C. Caughey, M. A. Farber, J. J. Fulton, P. F. Ford, W. A. Marston, R. Vallabhaneni, T. C. Nichols, and C. M. Gallippi, Ultrasound Med. Biol. **41**, 685 (2015).
[7] P. Dayton, A. Klibanov, G. Brandenburger, and K. Ferrara, Ultrasound Med. Biol. **25**, 1195 (1999).

[8] C. E. Owens, C. W. Shields, D. F. Cruz, P. Charbonneau, and G. P. López, Soft Matter **12**, 717 (2016).
[9] L. M. Johnson, L. Gao, C. W. Shields IV, M. Smith, K. Efimenko, K. Cushing, J. Genzer, and G. P. López, J. Nanobiotechnology **11**, 22 (2013).
[10] C. W. Shields, L. M. Johnson, L. Gao, and G. P. López, Langmuir **30**, 3923 (2014).
[11] T. Laurell, F. Petersson, and A. Nilsson, Chem. Soc. Rev. **36**, 492 (2007).
[12] S. D. Danilov and M. A. Mironov, Sov. Phys. Acoust. **30**, 280 (1984).
[13] A. A. Doinikov, J. Fluid Mech. **267**, 1 (1994).
[14] M. Settnes and H. Bruus, Phys. Rev. E **85**, (12 pages) (2012).
[15] P. H. Mott, J. R. Dorgan, and C. M. Roland, J. Sound Vib. **312**, 572 (2008).
[16] L. V. King, Proc. R. Soc. A Math. Phys. Eng. Sci. **147**, 212 (1934).
[17] K. Yosioka and Y. Kawasima, Acustica **5**, 167 (1955).
[18] T. Laurell and A. Lenshof, editors , *Microscale Acoustofluidics* (Royal Society of Chemistry, Cambridge, 2014).
[19] A. Doinikov, Phys. Rev. E **54**, 6297 (1996).
[20] P. V Chitnis, P. Lee, P. A. Dayton, J. Mamou, and J. A. Ketterling, Bubble Sci. Eng. Technol. **3**, 73 (2011).
[21] C. W. Shields IV, D. Sun, K. A. Johnson, K. A. Duval, A. V. Rodriguez, L. Gao, P. A. Dayton, and G. P. López, Angew. Chemie - Int. Ed. **53**, 8070 (2014).
[22] T. G. Mason, Rheol. Acta **39**, 371 (2000).
[23] E. Meijering, O. Dzyubachyk, and I. Smal, Methods Enzymol. **504**, 183 (2012).

TABLE I. A summary of assumptions and limiting cases of theoretical equations modeling the acoustic radiation force on compressible, spherical particles.

Theory	Particle Assumptions	Host Media Assumptions	Limiting Cases
Eq. (1) King [16]	Incompressible	Inviscid	$k_0R << 1$
Eq. (2) Yosioka and Kawasima [17]	Compressible	Inviscid	$(k_0R)^2$, $(k_pR)^2 << 1$
Eq. (3) Danilov and Mironov [12]	Compressible	Viscous	$R << \lambda_s$
Eq. (4) Doinikov [13]	Compressible	Viscous	$\delta_v << R << \lambda_s$
Eq. (5) Settnes and Bruus [14]	Compressible	Viscous	δ_v, $R << \lambda_s$

TABLE II. The Reynolds number (Re), acoustic wavelength (λ_s), viscous penetration depth (δ_v) and k_0R to determine the limiting cases of the experimental conditions of frequency (f), radius (R) and kinematic viscosity (v).

Independent Variable	f [MHz]	R [μm]	v [m^2/s]	Re	λ_s [μm]	δ_v [μm]	k_0R	Quantitative Analysis: Best Predictor
Frequency	1.0	1.05	1.01e-06	6.19e-04	1500	0.567	4.45e-03	Eq. (4) [13]
	2.5			7.81e-04	600	0.359	1.11e-02	
	5.0			9.28e-04	300	0.254	2.23-02	
	7.5			1.94e-03	200	0.207	3.34e-02	
Particle Size	7.5	1.05	1.01e-06	1.94e-03	200	0.207	3.34e-02	Eq. (3) [12]
		2.76		8.95e-03			8.78e-02	
		4.02		1.07e-02			1.28e-01	
Host Fluid Viscosity	7.5	1.05	1.01e-06	1.94e-03	200	0.207	3.34e-02	Eq. (5) [14]
			1.51e-06	1.24e-03		0.253		
			2.61e-06	3.47e-04		0.333		
			3.17e-06	3.05e-04		0.367		

TABLE III. The dependence of each theory on frequency, radius and viscosity.

Theory	Frequency	Radius	Viscosity
Eq. (2) Yosioka and Kawasima [17]	ω^4	R^6	N/A
Eq. (3) Danilov and Mironov [12]	$\omega^{3/2}$	R	ν
Eq. (4) Doinikov [13]	$\omega^{1/2}$	R^2	$\nu^{1/2}$
Eq. (5) Settnes and Bruus [14]	ω	R^3	$\frac{\nu}{\nu^{1/2}+\nu+\nu^{3/2}+\nu^2}$

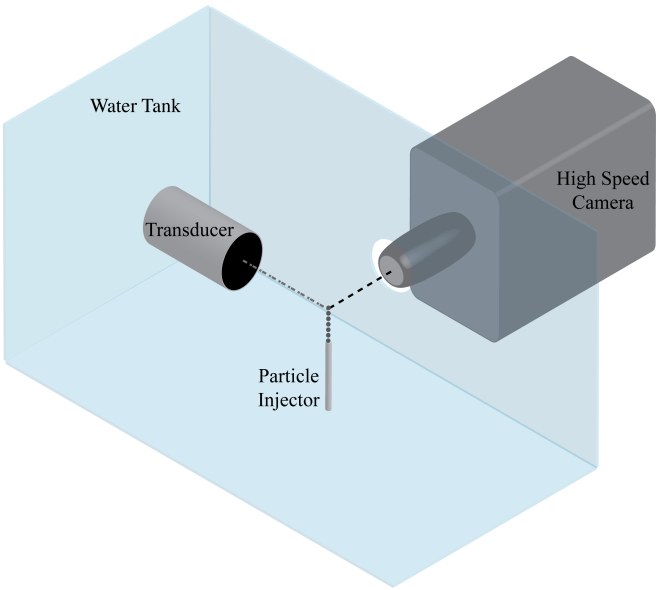

FIG 1. A schematic of opto-acoustic experimental setup to illustrate the mutual focal point of the camera lens, transducer and particle injector inside the water tank (not to scale).

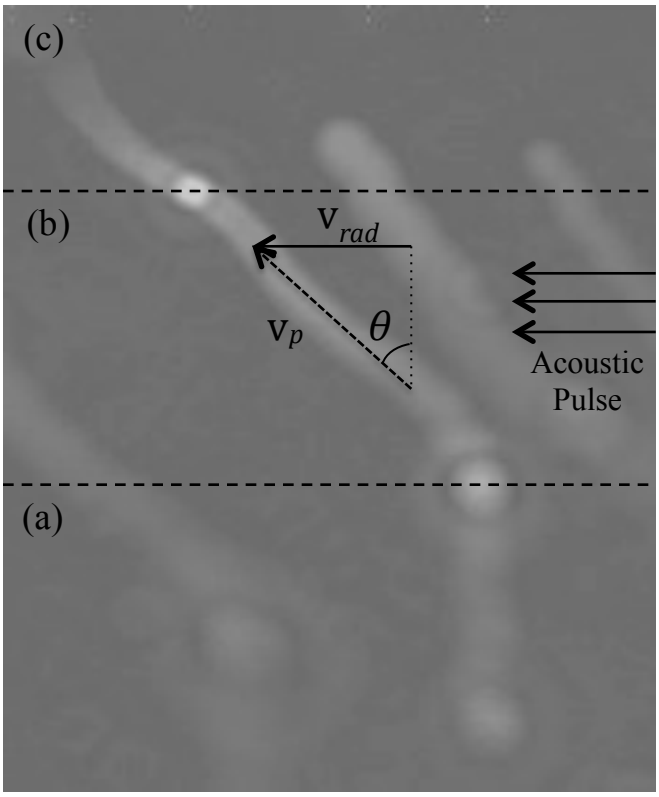

FIG 2. A representative composite time projection image of particle migration as it (a) emerges into the optical field in the absence of an acoustic pulse, (b) is deflected from its initial path by an acoustic pulse and (c) continues moving upward once the acoustic pulse is terminated.

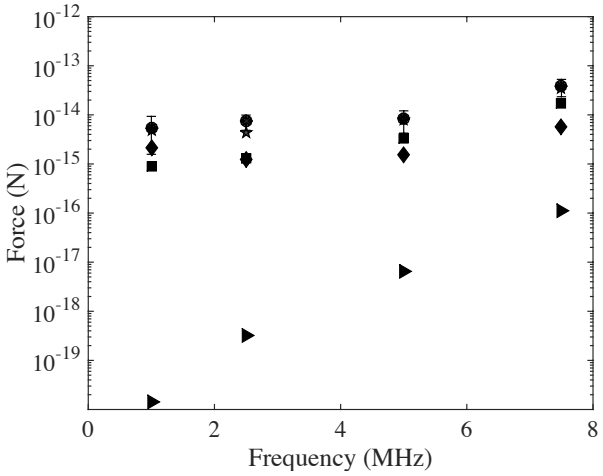

FIG 3. Acoustic radiation force vs. frequency for 2.1 μm diameter polystyrene particles in water; ▶, Eq. 2 (Yosioka and Kawasima [17]); ◆, Eq. 3 (Danilov and Mironov [12]); ★, Eq. 4 (Doinikov [13]); ■, Eq. 5 (Settnes and Bruus [14]); ●, experimental data.

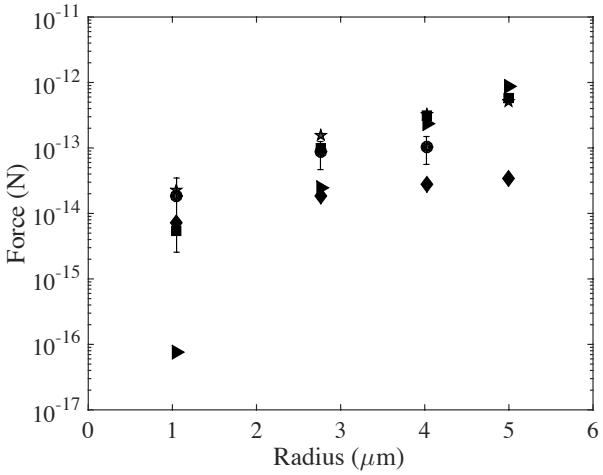

FIG 4. Acoustic radiation force vs. particle radius for polystyrene particles in water using a pulse from a 7.5 MHz ultrasound transducer; ▶, Eq. 2 (Yosioka and Kawasima [17]); ◆, Eq. 3 (Danilov and Mironov [12]); ★, Eq. 4 (Doinikov [13]); ■, Eq. 5 (Settnes and Bruus [14]); ●, experimental data.

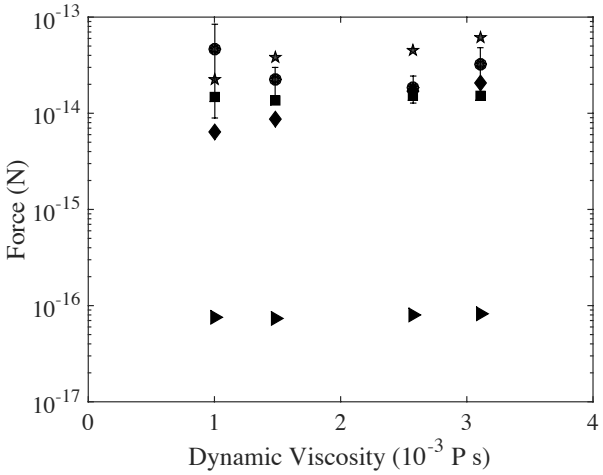

FIG 5. Acoustic radiation force vs. host media viscosity for 2.1 μm diameter polystyrene particles using a pulse from a 7.5 MHz ultrasound transducer; ▶, Eq. 2 (Yosioka and Kawasima [17]); ◆, Eq. 3 (Danilov and Mironov [12]); ★, Eq. 4 (Doinikov [13]); ■, Eq. 5 (Settnes and Bruus [14]); ●, experimental data.